Halide Binding by the D212N Mutant of Bacteriorhodopsin Affects Hydrogen Bonding of Water in the Active Site†

Mikihiro Shibata,‡ Maiko Yoshitsugu,‡ Noriko Mizuide,‡ Kunio Ihara,§ and Hideki Kandori*,‡

Department of Materials Science and Engineering, Nagoya Institute of Technology, Showa-ku, Nagoya 466-8555, Japan, and Graduate School of Science, Nagoya University, Chikusa-ku, Nagoya 454-8602, Japan

Received March 1, 2007; Revised Manuscript Received April 24, 2007

ABSTRACT: Bacteriorhodopsin (BR), a membrane protein found in *Halobacterium salinarum*, functions as a light-driven proton pump. The Schiff base region has a quadrupolar structure with positive charges located at the protonated Schiff base and Arg82, and the counterbalancing negative charges located at Asp85 and Asp212. The quadropole inside the protein is stabilized by three water molecules, forming a roughly planar pentagonal cluster composed of these waters and two oxygens of Asp85 and Asp212 (one from each carboxylate side chain). It is known that BR lacks proton-pumping activity if Asp85 or Asp212 is neutralized by mutation, but binding of Cl^- has different functional effects in mutants at these positions. Binding of Cl^- to D85T converts into a chloride ion pump (Sasaki, J., Brown, L. S., Chon, Y.-S., Kandori, H., Maeda, A., Needleman, R., and Lanyi, J. K. (1995) *Science 269*, 73−75). On the other hand, photovoltage measurements suggested that binding of Cl^- to D212N restores the proton-pumping activity at low pH (Moltke, S., Krebs, M. P., Mollaaghababa, R., Khorana, H. G., and Heyn, M. P. (1995) *Biophys. J. 69*, 2074−2083). In this paper, we studied halide-bound D212N mutant BR in detail. Light-induced pH changes in a suspension of proteoliposomes containing D212N(Cl^-) at pH 5 clearly showed that Cl^- restores the proton-pumping activity. Spectral blue-shift induced by halide binding to D212N indicates that halides affect the counterion of the protonated Schiff base, whereas much smaller halide dependence of the λ_{max} than in D85T suggests that the binding site is distant from the chromophore. In fact, the K minus BR difference Fourier-transform infrared (FTIR) spectra of D212N at 77 K exhibit little halide dependence for vibrational bands of retinal and protein. The only halide-dependent bands were the C═N stretch of Arg82 and some water O−D stretches, suggesting that these groups constitute a halide-binding pocket. A strongly hydrogen-bonded water molecule is observed for halide-bound D212N, but not for halide-free D212N, which is consistent with our hypothesis that such a water molecule is a prerequisite for proton-pumping activity of rhodopsins. We concluded that halide binding near Arg82 in D212N restores the water-containing hydrogen-bonding network in the Schiff base region. In particular, the ion pair formed by the Schiff base and Asp85 through a strongly hydrogen-bonded water is essential for the proton-pumping activity of this mutant and may be controlled by the halide binding to the distant site.

Bacteriorhodopsin (BR[1]) functions as a light-driven proton pump in *Halobacterium salinarum* (*1*, *2*). The chromophore of this protein is all-*trans*-retinal that binds to a lysine residue through a Schiff base linkage, and the all-*trans* to 13-*cis* photoisomerization triggers the photocycle for proton pump (*2*). The photocycle comprises a series of intermediates, designated as the J, K, L, M, N, and O states. BR is the best studied molecular pump, where various methods have been applied (*3*−*5*), and mechanisms for unidirectional translocation of protons have been established (*1*, *2*).

The essential parts of the proton-pumping mechanism have been examined by mutagenesis. For example, Asp96 on the cytoplasmic side is a proton donor for the Schiff base in the M to N transition, but it is known that the D96N mutant pumps protons (*6*). Glu204 and Glu194 constitute a proton release group in the extracellular side, but it is also known that the E204Q and E194Q mutants pump protons (*6*). These facts indicate that terminal protonatable groups, such as Asp96 and Glu204/Glu194, are not essential for the proton-pumping mechanism in BR. In contrast, D85N and D212N mutants in the Schiff base region lack proton-pumping activity at neutral pH (*7*). Therefore, the Schiff base region constitutes the "switch" of the pumping function in BR (*8*). Figure 1 illustrates the Schiff base region of BR (*9*). It contains a quadrupole with positive charges located at the protonated Schiff base and Arg82, and the counterbalancing negative charges located at Asp85 and Asp212. The quadrupole inside the protein is stabilized by three water molecules (water401, 402, and 406). The Schiff base region contains a roughly planar pentagonal cluster, which is

† This work was supported by grants from Japanese Ministry of Education, Culture, Sports, Science, and Technology to H.K. (15076202) and Research Fellowships from the Japan Society for the Promotion of Science for Young Scientists to M.S.

* To whom correspondence should be addressed. Phone and fax: 81-52-735-5207. E-mail: kandori@nitech.ac.jp.

‡ Nagoya Institute of Technology.

§ Nagoya University.

[1] Abbreviations: BR, bacteriorhodopsin; *p*HR, *pharaonis* halorhodopsin; FTIR, Fourier-transform infrared; 5-FOA, 5-fluoroorotate; CCCP, carbonyl cyanide *m*-chlorophenyl hydrazone.

10.1021/bi7004224 CCC: $37.00
Published on Web 06/05/2007

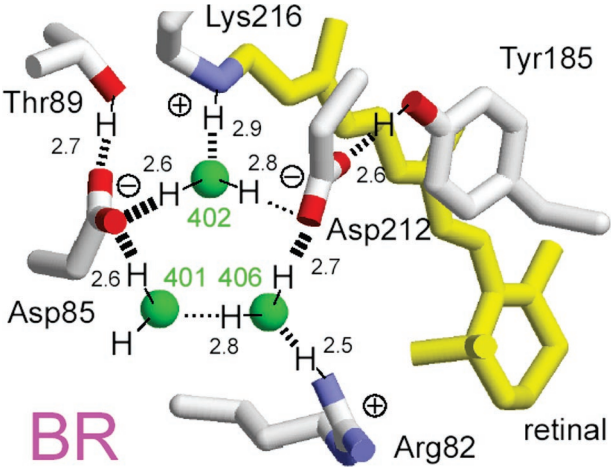

FIGURE 1: X-ray crystallographic structure of the Schiff base region in BR from PDB entry 1C3W (*9*). The membrane normal is approximately in the vertical direction of this figure. Upper and lower regions correspond to the cytoplasmic and extracellular sides, respectively. Green spheres (401, 402, and 406) represent water molecules in the Schiff base region. Position of hydrogen atoms of water and their hydrogen-bonding strengths (dotted lines) are obtained from our previous FTIR study (*24*), where thick dotted lines correspond to strong hydrogen bonds.

composed by three water oxygens and two oxygens from Asp85 and Asp212 (one from each side chain).

Asp85 and Asp212 are located at a similar distance from the Schiff base, whereas the Schiff base proton is transferred to only Asp85 in the L to M transition (*10*). As described above, neutralization of these aspartates (D85N and D212N) abolishes the proton-pumping activity. Interestingly, replacement of Asp at position 85 by Thr or Ser converts BR into a Cl^- pump (*11*, *12*). Although Cl^- binding affinity is very low for D85N, it can also bind Cl^- at low pH (*13*). In the absence of Cl^-, the absorption maximum of D85N is located at ~600 nm, but Cl^- binding shifts the absorption maximum to ~570 nm, because Cl^- becomes the counterion of the protonated Schiff base (*13*). On the other hand, the absorption maximum of D212N is located at ~580 nm at pH >7 (*14*), suggesting that Asp212 is a weaker counterion than Asp85. The M intermediate is not formed during the photocycle, even though there are a proton donor (protonated Schiff base) and an acceptor (Asp85) in D212N. In the presence of Cl^- at low pH, D212N has a purple color similar to the wild-type. Photovoltage measurements suggested that D212N does not pump Cl^-, but the proton-pumping activity seems to be restored (*15*). These results imply different roles of two aspartates at positions 85 and 212, which cannot be predicted from the structure in Figure 1.

Fourier-transform infrared (FTIR) spectroscopy is a powerful tool to investigate the detailed structure and structural changes in the active center of rhodopsins (*5*, *8*). In particular, N−H and O−H stretching vibrations at 3800−2700 cm^{-1} (N−D and O−D stretches at 2700−2000 cm^{-1} in D_2O) directly monitor their hydrogen bonds (*16*). By means of low-temperature FTIR spectroscopy, we have identified these vibrations in the Schiff base region of BR, which involve the N−D stretch of the Schiff base (*17*), the O−D stretch of Thr89 (*18*−*20*), the N−D stretch of Arg82 (*21*), and O−D stretches of water molecules (*22*−*25*). They provided useful information on how the hydrogen-bonding network of the Schiff base region is altered in the photocycle. For example, the N−D stretch of the Schiff base is upshifted by 350 cm^{-1} by retinal photoisomerization (*17*), indicating that the Schiff base loses a hydrogen bond with water402 (Figure 1) upon the retinal rotation around the C13═C14 bond. Although water402 looks symmetrically positioned relative to Asp85 and Asp212 in Figure 1, comprehensive mutation study revealed that water402 forms a strong hydrogen bond with Asp85 (O−D stretch at 2171 cm^{-1}), but interacts with Asp212 weakly (O−D stretch at 2636 or 2599 cm^{-1}) (*24*). This means that water402 bridges the Schiff base and Asp85, but not Asp212. On the basis of this assignment, we proposed that hydration switch of water402 from Asp85 to Asp212 leads to the primary proton transfer from the Schiff base to Asp85 upon formation of the M intermediate (*26*). The hydration switch model could explain the reason why D212N lacks proton-pumping activity despite the presence of the proton donor (protonated Schiff base) and the acceptor (Asp85), as association of water402 to neutral Asn212 is not sufficient to drive the proton transfer.

In addition, a strong hydrogen bond of water402 to Asp85 in the unphotolyzed state is important for the proton-pumping activity of BR. Among various BR mutants tested, only D85N and D212N lack strongly hydrogen-bonded water molecules (O−D stretch at <2400 cm^{-1}) and proton-pumping activity (*23*, *24*). Not only D85N but also the chloride-pumping D85S does not possess such strongly hydrogen-bonded water molecules (*27*). Therefore, we inferred that the presence of a strong hydrogen bond of water is a prerequisite for proton pumping in BR (*28*). Interestingly, this hypothesis is true not only for the mutants of BR but also for other archaeal rhodopsins (*29*−*32*), archaeal-type rhodopsins from eubacteria (*33*−*35*) and eukaryotes (*36*, *37*). It is likely that the proton-pumping rhodopsins stabilize water molecule(s) in the Schiff base region by strong hydrogen bonding with its counterion such as Asp85, and light-induced destabilization of the hydrogen bond of such water contributes to the energy storage for driving the proton pump. If D212N pumps protons upon binding of chloride, we expect the presence of strongly hydrogen-bonded water molecule(s) according to the hypothesis.

FTIR spectroscopy can also study the environment of chloride, because the halide dependence (Cl^-, Br^-, and I^-) of the spectral features provides detailed structural information of the binding site. By revealing no halide dependence of the N−D stretching vibration of the Schiff base and O−D stretching vibration of water molecules in the L_1 intermediate of *pharaonis* halorhodopsin (*p*HR), we were able to propose a new model of the early stage of chloride transport (*31*). According to the model, removal of the hydrogen bonds with the Schiff base and water(s) makes the environment around chloride less polar in the L_1 intermediate, which drives the motion of chloride. On the other hand, clear halide dependence was observed for the N−D stretch of the Schiff base in the halide-bound D85S, implying that halide is a hydrogen-bonding acceptor of the Schiff base (*27*).

In this article, we studied the halide-bound D212N mutant of BR, particularly from the structural point of view. We first measured the proton-pumping activity of D212N by use of proteoliposomes. Light-induced pH changes clearly showed the proton-pumping activity of D212N(Cl^-). Visible absorption spectra of halide-bound D212N showed small halide

dependence. The K minus BR difference infrared spectra of D212N at 77 K exhibit little halide dependence for vibrational bands of retinal and protein. Almost no halide dependence of the Schiff base vibrations strongly suggests that halide is not a direct hydrogen-bonding acceptor of the Schiff base, unlike in D85S. On the other hand, halide-dependent bands observed exclusively for C=N stretch of Arg82 and some water O−D stretches suggested that these groups constitute the halide-binding pocket. A strongly hydrogen-bonded water molecule is observed for the halide-bound D212N, but not for the halide-free D212N, which is consistent with our hypothesis that such a water molecule is a prerequisite for proton-pumping activity of rhodopsins. We concluded that halide binding near Arg82 in D212N restores the water-containing hydrogen-bonding network in the Schiff base region.

MATERIALS AND METHODS

Plasmid Constructs and Site-Directed Mutagenesis. A fragment containing the *bop* gene (1.6 kbp) was amplified by PCR and cloned into the vector pGEM-T easy (Promega) using the primer set (5′-ggatccGACGTGAAGATGGGGC-3′, 5′-ggatccGTGACCGTTCGATGC-3′). A cloned fragment was confirmed by sequencing and then transferred to the vector pUC18 for mutagenesis, or the vector pMPK54 for transformation (*38*), which contains a gene conferring resistance to the 3-hydroxy-3-methylglutaryl CoA reductase inhibitor simvastatin in *H. salinarum*. A point mutation (Asp212 → Asn) was introduced into the *bop* gene by PCR mutagenesis (Stratagene), and resultant mutation was confirmed by sequencing the plasmids prior to transformation of *H. salinarum*.

Transformation for H. salinarum. *H. salinarum* strain MPK409 (*38*) was transformed using the plasmid described above. The transformation procedure was essentially as described in a previous paper (*39*). Briefly, 10 mL of early log phase cells were collected by centrifugation (6000*g*, 10 min) and resuspended in 2 mL of spheroplasting solution. 100 μL aliquots were added to 10 μL of 0.5 M EDTA in spheroplasting solution and gently mixed. After 20 min, 3−5 μg of plasmid DNA in 10 μL was added and incubated for a further 10 min. An equal volume (120 μL in this case) of 60% polyethylene glycol 600 in spheroplasting solution was added and mixed gently tilting the tube back and forth. After 20 min of additional incubation, 1 mL of regeneration salt solution was added. Cells were pelleted in a microcentrifuge at 5000 rpm for 5 min, and 1 mL of complex culture medium containing 15% sucrose was added to the resultant pellet. After incubation for 48 h at 37 °C, 100 μL samples were spread on plates containing 15% sucrose and 10 μg/mL simvastatin. After 10 days of incubation at 40 °C, purple colored colonies were picked and grown in complex cuture medium with 10 μg/mL simvastatin, and after incubation for 24 h at 37 °C, 100 μL samples were spread on plates containing 250 μg/mL 5-FOA. After a week of incubation, purple colonies were picked and grown again in complex cuture medium containing 50 μg/mL uracil. The purple membranes were isolated and purified in the usual manner (*40*).

Light-Induced pH Changes. Liposomes were prepared by sonication for 10 min at 4 °C with desiccated lipids (L-α-phosphatidylcholine, type IV-S) and 0.5 mM MOPS buffer (containing 2 M NaCl and 50 mM Mg_2SO_4, pH 7.5). Proteoliposomes were reconstituted by sonication of a mixture of liposomes and PM for 5 min (*41*). The lipid/BR (w/w) ratio was about 50 for both the wild-type and D212N. pH changes in suspension of proteoliposomes were measured by glass electrode under illumination at >500 nm (30 °C) by use of a HORIBA F-55 pH meter. The samples were then illuminated after addition of CCCP to a final concentration of 10 μM. Proton-pumping activities were calculated by adding 10 μL of 0.01 N HCl to the suspension.

UV−Visible Spectroscopy. Absorption spectra of D212N in the absence and presence of halides were measured for the purple membrane suspension containing the D212N protein at 20 °C by use of a SHIMADZU UV-2400PC UV−visible spectrometer. Each sample contains 50 mM Na_2SO_4 (2 mM boric acid buffer pH 10), 150 mM NaCl, NaBr, or NaI (2 mM citric acid buffer pH 5).

HPLC Analysis. HPLC analysis was performed as described previously (*34*). Light-adapted D212N was prepared by illuminating the sample with >500 nm light, while dark-adapted D212N was prepared by keeping the samples in the dark overnight at 4 °C. Extraction of retinal oxime from the sample was carried out by hexane after denaturation by methanol and 500 mM hydroxylamine at 4 °C. Three independent measurements were averaged, where experimental accuracy was within 1.0% for light-adapted D212N, and within 3.0% for dark-adapted D212N.

FTIR Measurements. The sample films of halide-bound and halide-free D212N were prepared by drying the purple membrane suspension in 2 mM citric acid buffer (pH 5) containing 5 mM NaCl, NaBr, or NaI, and in 2 mM boric acid buffer (pH 10) containing 1.6 mM Na_2SO_4, respectively, on a BaF_2 window with a diameter of 18 mm. The films were then hydrated by 1 μL of H_2O, D_2O, or $D_2{}^{18}O$, and the sample was placed in a cell and then the cell mounted in an Oxford DN-1704 cryostat. The hydrated film was illuminated with >500 nm light for 1 min at 273 K to obtain the light-adapted state of D212N. Low-temperature FTIR spectroscopy was applied as described previously by use of a Bio-Rad FTS-40 FTIR spectrometer (*16*−*20*). The K minus BR spectra were measured by photoconversion between K and BR at 77 K. Each spectrum was normalized to that of D212N(Cl^-) at the negative 1203 cm^{-1} band corresponding to a C−C stretch of the retinal chromophore. The normalization factors were 0.95 for D212N(free) and D212N(Br^-), 2.0 for D212N(I^-), 2.6 for D85S(Cl^-) and D85S(Br^-), 3.4 for D85S(I^-), and 0.4 for the wild-type. The spectra of the wild-type and D85S mutant were reproduced from refs 23 and 27, respectively.

RESULTS

Measurement of Proton Transport in BR Liposomes. Light-driven proton transport was measured for proteoliposomes of D212N(Cl^-) by monitoring the pH changes with a glass electrode. Figure 2 shows light-induced pH changes of proteoliposomes containing the wild-type or D212N. In the case of the wild-type at pH 7, illumination caused a net alkalization of the medium, indicating that protons are pumped toward inside the liposomes. Addition of 10 μM CCCP abolished the observed light-induced pH changes (data

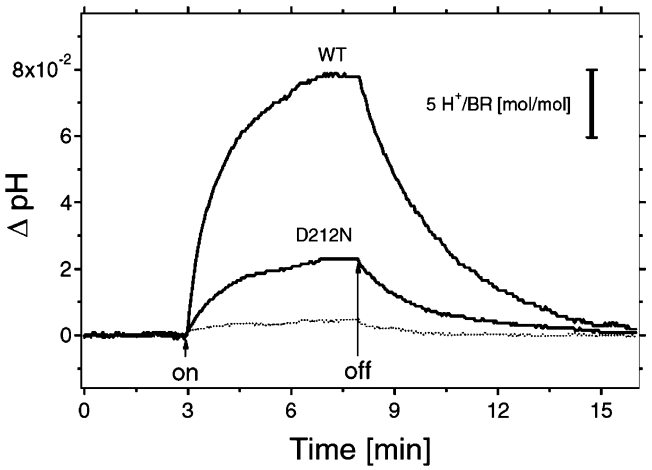

FIGURE 2: Time course of light-induced alkalization by proteoliposomes containing D212N (0.5 mM citric acid at pH 5) or the wild-type BR (0.5 mM MOPS at pH 7) under continuous illumination at >500 nm. Both D212N and the wild-type samples contain 2 M NaCl. After addition of 10 μM CCCP, the signal was almost abolished (dotted line) for D212N.

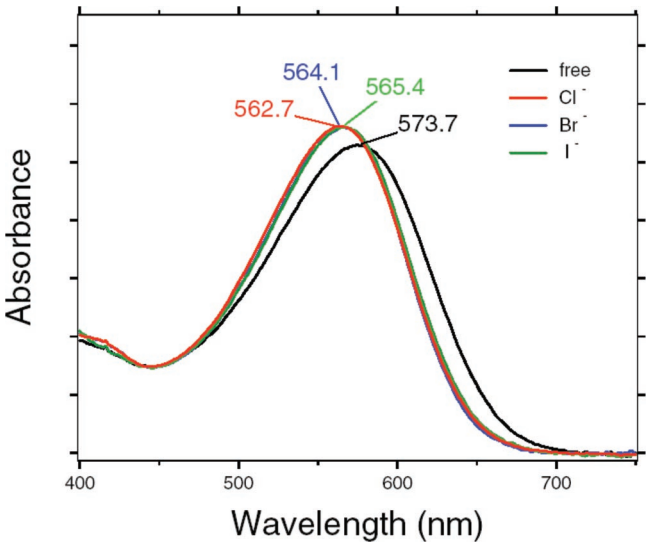

FIGURE 3: Absorption spectra of halide-free (black line), Cl^--bound (red line), Br^--bound (blue line), and I^--bound (green line) D212N BR in the purple membrane suspension at 20 °C. Halide-bound forms were obtained in the presence of 150 mM halides at pH 5. One division of the *y*-axis corresponds to 0.1 absorbance unit.

not shown). It is known that BR molecules reconstituted at neutral pH prefer an inside-out orientation in liposomes, so that illumination causes a net alkalization (*41*). Therefore, the present study reproduced the previous report for the wild-type BR.

In the case of D212N at pH 5, illumination caused a net alkalization similar to the wild-type (Figure 2). Addition of 10 μM CCCP abolished the observed light-induced pH changes (dotted line in Figure 2), which is completely opposite to the effect expected for a chloride pump (*42*). Similar pH changes for the wild-type and D212N strongly suggest that D212N pumps protons in the presence of chloride. We also observed significant reduction of the pH changes for D212N at pH 7 (data not shown), where chloride binding is decreased. Thus, the present results show that D212N pumps protons in the presence of chloride, as is suggested by the previous photovoltage measurements (*15*).

Absorption Spectra of the D212N Mutant in the Presence of Halides. Figure 3 shows visible absorption spectra of the light-adapted D212N in the purple membrane suspension. In the absence of halides, the absorption maximum is located at 573.7 nm (pH 10; black line in Figure 3). The absorption spectrum is similar for the halide-free D212N at pH 5. Addition of halides (at pH 5) shifts the absorption spectra to shorter wavelengths, with the λ_{max} located at 563−565 nm. This fact indicates that halides affect the Schiff base counterion (*14*). Despite the spectra looking almost identical among the three halides, we noted that the λ_{max} is at 562.7 nm for Cl^-, 564.1 nm for Br^-, and 565.4 nm for I^-. A previous study reported that the λ_{max} values of D85T are located at 555−566 nm for the same three halides (*43*). Therefore, the halide dependence of the λ_{max} for the D212N mutant (difference of 2.7 nm) is much smaller than that for D85T (11 nm). The X-ray crystallographic structure of D85S(Br^-) reported that Br^- is the direct hydrogen-bonding acceptor of the Schiff base (*44*). In contrast, halides probably bind to the Schiff base region of D212N in a manner different from being a direct hydrogen-bonding acceptor of the Schiff base. Consequently, halides act as a weaker counterion of the protonated Schiff base.

Table 1: Isomeric Composition (%) of the Retinal Chromophore by the HPLC Analysis of D212N

	light−adapted		dark−adapted	
	all-*trans*	13-*cis*	all-*trans*	13-*cis*
free	94	6	35	65
Cl^-	94	6	50	50
Br^-	94	6	64	36
I^-	94	6	63	37

It should be noted that the previous report on the λ_{max} of halide-bound D212N was different from the present observation. Marti et al. reported that the λ_{max} is at 545 nm (Cl^-), 544 nm (Br^-), and 535 nm (I^-) (*45*), with the halide dependence opposite to the present study. They expressed D212N in *Escherichia coli*, and it is known that various properties of BR can be modified compared to the native state that is expressed in *Halobacterium salinarum*. In particular, the phenotype of the Asp212 mutant is significantly influenced by the expression conditions, which was pointed out by Needleman et al. (*14*) and Krebs et al. (*46*). Marti et al. reported that the light-adapted D212N contains 5% 9-*cis* and 11% 11-*cis* retinal by HPLC analysis (*45*), which may indicate unusual protein folding and/or photocycle. We thereby measured isomeric composition of the retinal chromophore of D212N in the presence of various halides. Table 1 shows that the observed retinal isomers were only all-*trans* and 13-*cis* forms both for the dark-adapted and light-adapted D212N. Thus, the present HPLC analysis emphasizes the importance of the expression in *H. salinarum*, not in *E. coli*, particularly in the study of the D212N mutant. Table 1 also shows that D212N undergoes light adaptation like the wild-type, and the light-adapted D212N contains 94% all-*trans* form in the absence and presence of various halides. From the HPLC analysis, we can safely state that the small difference in the λ_{max} in Figure 3 does not originate from the different isomeric ratios.

K Minus BR Difference Infrared Spectra for D212N in the 1800−900 cm^{-1} Region. Visible spectral analysis of the halide-bound D212N suggests that halide binds to the Schiff

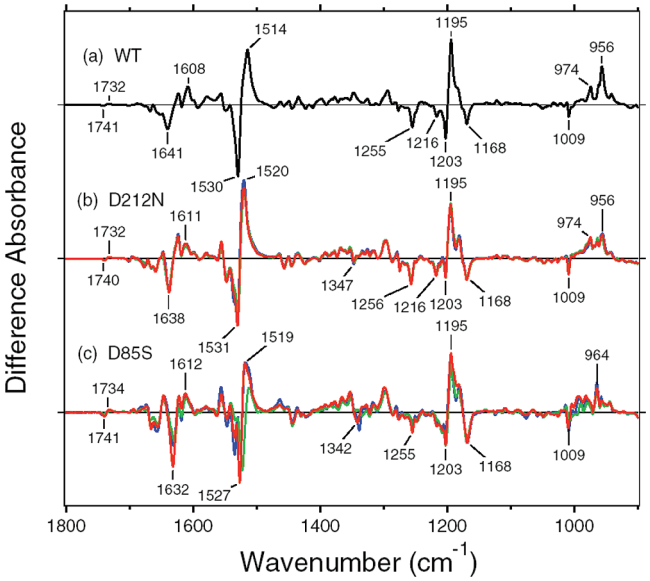

FIGURE 4: The K minus BR difference infrared spectra of the wild-type (a), D212N (b), and D85S (c) in the presence of Cl^- (red), Br^- (blue), and I^- (green) in the 1800−900 cm^{-1} region. The samples were hydrated with H_2O, the spectra for the wild-type and D212N were measured at 77 K, and the spectra for D85S were measured at 130 K. Parts of the spectra of the wild-type (*16*) and halide-bound D85S (*27*) were published previously. One division of the *y*-axis corresponds to 0.035 absorbance unit.

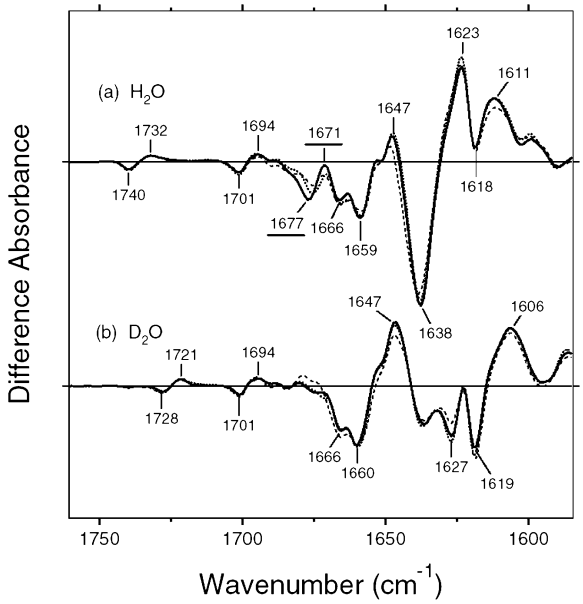

FIGURE 5: The K minus BR difference infrared spectra of D212N in the presence of Cl^- (solid lines), Br^- (dotted lines), and I^- (broken lines) at pH 5 in 1760−1585 cm^{-1} region. The samples were hydrated with H_2O (a) and D_2O (b), and spectra were measured at 77 K. Underlined frequencies (1677 (−)/1671 (+) cm^{-1}) show clear halide dependence. One division of the *y*-axis corresponds to 0.012 absorbance unit.

base region, but not in a hydrogen-bonding acceptor position. This is different from the mutant of Asp85, where halide is a direct hydrogen-bonding acceptor of the Schiff base as was shown for D85S(Br^-) (*44*). To further study the structure of the halide binding site, we measured FTIR difference spectra of the halide-bound D212N. Figure 4 compares halide-dependent K minus BR difference spectra of the wild-type (a), D212N (b), and D85S (c) in the 1800−900 cm^{-1} region, which monitors local structure around the retinal chromophore at cryogenic temperatures. It is clearly seen that there is little halide dependence for D212N (Figure 4b). In contrast, the spectra are considerably different among the three halide-bound forms of D85S (Figure 4c). According to the X-ray structure of D85S(Br^-) (*44*), Br^- is located at the position of water402 in the wild-type BR (Figure 1), so that Br^- is the direct hydrogen-bonding acceptor of the Schiff base. Therefore, it is reasonable to expect that a difference in the nature of the bound halide will affect the K minus BR spectra significantly. Similarity of the spectra of D212N (Figure 4b) to the wild-type (Figure 4a) as well as little halide dependence are fully consistent with the conclusion from visible absorption spectra that halide is not in a hydrogen-bonding acceptor position.

The largest bands at 1531 (−)/1520 (+) cm^{-1} in Figure 4b probably originate from ethylenic C═C stretching vibrations of the retinal chromophore. A spectral downshift indicates formation of the red-shifted K-intermediate in D212N. No clear halide dependence was observed for the band, though it is known that the band is correlated to the visible absorption spectra (Figure 3). The reason may be due to the insufficient spectral resolution (2 cm^{-1}) of the present FTIR measurements. The 1250−1150 cm^{-1} region monitors C−C stretching vibrations of the retinal chromophore. Like in the wild-type (Figure 4a), negative bands at 1256, 1216, 1203, and 1168 cm^{-1} are attributable to the C−C stretching vibrations of the retinal chromophore at position C12−C13, C8−C9, C14−C15, and C10−C11, respectively (*47*). A positive 1195 cm^{-1} band of the K-intermediate originates from the C14−C15 and C10−C11 stretches. Similarity of the spectra of halide-bound D212N (Figure 4b) to that of the wild-type (Figure 4a) suggests that the retinal isomerization occurs from the all-*trans* to the 13-*cis* form. The absence of halide dependence implies that halides play an insignificant role in the retinal photoisomerization in D212N. It is also the case for the hydrogen out-of plane (HOOP) vibrations of the retinal chromophore in the 1100−900 cm^{-1} region. HOOP modes are sensitive to chromophore distortions, particularly in the K state, and unlike for D85S (Figure 4c), the absence of halide dependence shows that halide hardly affects the retinal photoisomerization in D212N (Figure 4b). In summary, vibrations of the retinal chromophore such as C═C and C−C stretches and HOOP modes are not affected by the variation in halide size. Therefore, we infer that halides bind to the region distant from the retinal chromophore. We note that, although the bands characterizing the retinal chromophore are not affected by the halide, other bands exhibited in the 1760−1585 cm^{-1} region shows halide dependence (Figure 5).

K Minus BR Difference Infrared Spectra for D212N in the 1760−1585 cm^{-1} Region. Figure 5 shows the K minus BR difference infrared spectra of halide-bound D212N in the 1760−1585 cm^{-1} region at 77 K. This frequency region monitors vibrations of protein except for the C═N stretch of the chromophore. The similarity of the spectra suggests small halide effect on these molecular vibrations. The bands at 1740 (−)/1732 (+) cm^{-1} (Figure 5a) downshift to 1728 (−)/1721 (+) cm^{-1} in D_2O (Figure 5b), which can be identified as the C═O stretch of Asp115 because of the similar band in the wild-type (*10*). The bands of Asp115 were not affected by halides. The bands at 1701 (−)/1694

(+) cm^{-1} are interesting. The K minus BR spectra of the wild-type also possess the negative band at about 1701 cm^{-1} (*16*), but the amplitude of the negative 1701 cm^{-1} band is about 3 times larger in D212N than in the wild-type (data not shown). The K minus BR spectra of the wild-type has no positive band at about 1694 cm^{-1} (*16*). Since they are not sensitive to D_2O hydration (Figure 5b), they may originate from the C=O stretch of Asn212. If this is the case, the hydrogen bond of the C=O group of Asn212 is strengthened upon K formation. Interestingly, no halide dependence was observed for the bands. Therefore, we may conclude that halide does not bind in the vicinity of Asn212 in D212N.

Only the bands at 1677 (−)/1671 (+) cm^{-1} in D212N(Cl^-) exhibit halide dependence in this frequency region (Figure 5a), suggesting that the respective group belongs to the halide binding pocket. D212N(Br^-) and D212N(I^-) possess the negative band at 1675 and 1674 cm^{-1}, respectively. Since the bands disappear upon D_2O hydration (Figure 5b), it is unlikely that they can be ascribed to amide I vibrations. Braiman et al. reported that the C=N stretching vibration of arginine side chain appears in this region, and it downshifts by ~70 cm^{-1} upon deuteration (*48*). In addition, the C=N stretching vibration of arginine side chain in BR is observed at ~1660 cm^{-1} from time-resolved FTIR study of ^{15}N-labeled arginine (*49*). By use of mutant, they assigned the band to Arg82, which is located in the Schiff base region (Figure 1) (*50*). These facts strongly suggest that the halide-dependent bands at 1680−1670 cm^{-1} originate from the C=N stretching vibration of Arg82. Though not identified by isotope labeling in the present study, this is a reasonable interpretation because positively charged Arg82 is a good interaction partner of halide inside the protein.

The following bands are observed in the 1670−1600 cm^{-1} region: 1666 (−), 1659 (−), 1647 (+), 1638 (−), 1623 (+), 1618 (−), and 1611 (+) cm^{-1}. The negative 1666 cm^{-1} band appeared in the frequency of the amide I vibration of α_{II} helix, while the bands at 1659 (−)/1647 (+) cm^{-1} are assigned as the amide I vibration of α_I helix. No shift upon D_2O hydration (Figure 5b) is consistent with the assignment of amide I vibrations. The bands at 1623 (+)/1618 (−) cm^{-1} were previously assigned as the amide I vibration of Val49 for the wild-type (*51*). The spectral band of D212N at around 1620 cm^{-1} (Figure 5) is similar to that of the wild-type, suggesting that the same amide-I vibrations of Val49 are present in the spectra of D212N. No halide dependence was observed for these amide-I vibrations.

The bands at 1638 (−)/1611 (+) cm^{-1} probably originate from the C=N stretching vibration of the Schiff base, because they shift upon D_2O hydration. While the negative band was not uniquely determined (presumably at 1627−1618 cm^{-1}), the positive band at 1606 cm^{-1} is assignable as the C=ND stretch of the Schiff base in K in D_2O (Figure 5b). The absence of halide dependence should be also noted for these bands. We previously observed clear halide dependence for the C=N stretching vibrations of the Schiff base in the D85S mutant of BR (*27*), and we interpreted it as a direct interaction between the protonated Schiff base and halide by hydrogen bonding. Therefore, the absence of halide dependence for the C=N stretch of D212N can be interpreted in terms of the lack of a direct hydrogen bond between the Schiff base and halide, unlike in the D85S mutant. This interpretation is further tested by observing the N−D stretching vibration of the Schiff base in D_2O, which is a more direct probe of the hydrogen-bonding strength of the protonated Schiff base.

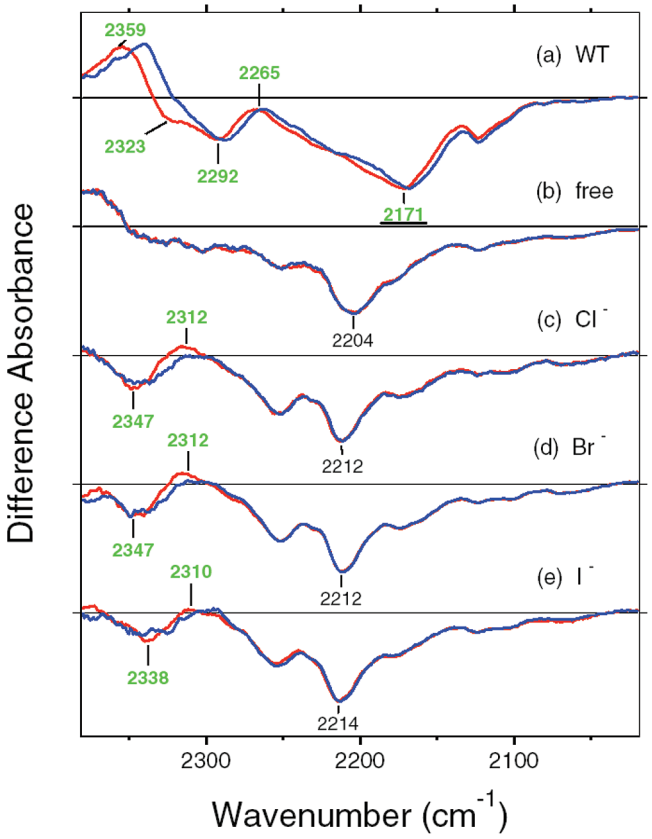

FIGURE 6: The K minus BR difference infrared spectra of the wild-type (a), halide-free (b), Cl^--bound (c), Br^--bound (d), and I^--bound (e) D212N in the 2380−2020 cm^{-1} region. The samples were hydrated with D_2O (red curves) or $D_2{}^{18}O$ (blue curves), and spectra were measured at 77 K. Green-labeled frequencies correspond to those identified as O−D stretching vibrations of water. The underlined frequency (2171 cm^{-1}) in the wild-type also contains the N−D stretch of the Schiff base (*17*). One division of the *y*-axis corresponds to 0.0017 absorbance unit.

X−D (N−D or O−D) Stretching Vibration Region of D212N in the Presence of Halides. In the 1800−800 cm^{-1} region, halide-dependent bands were only observed at 1680−1670 cm^{-1}, which is most likely to be the C=N stretch of Arg82. We next examined a higher frequency region, where the N−D stretch of the Schiff base and O−D stretches of water are observed in D_2O. The N−D stretch of arginine is also present in this region, as was shown for the wild-type BR (*21*). Figure 6 shows the K minus BR difference spectra in the 2380−2020 cm^{-1} region in D_2O. In the case of the wild-type BR, the bands at 2359 (+), 2323 (−), 2292 (−), 2265 (+), and 2171 (−) cm^{-1} (red curve in Figure 6a) are identified as O−D stretching vibrations of water molecules because of the spectral downshift in $D_2{}^{18}O$ (blue curve in Figure 6a) (*22*). From the frequency, these water molecules form a strong hydrogen bond (*22*), and comprehensive mutation study revealed that these water O−D stretches originate from three water molecules in the Schiff base region (Figure 1) (*24*). The negative 2171 cm^{-1} band also contains the N−D stretching vibration of the Schiff base, which was idenitifed by use of [ξ-^{15}N]Lys-labeled BR (*17*). The bands

at 2292 (−)/2265 (+) cm^{-1} also contain the N−D stretching vibrations of Arg82, which was identified by use of ^{15}N-Arg labeled BR (*21*).

The water bands completely disappeared in this frequency region upon the mutation of Asp212 (D212N) as shown by the identical red and blue curves (Figure 6b). We previously suggested that neutralization of Asp212 significantly perturbs the water-mediated hydrogen-bonding network in the Schiff base region, so that hydrogen bonds of water are weakened. Figure 6b shows a negative peak at 2204 cm^{-1}, which is most likely to be the N−D stretch of the Schiff base. The frequency similar to that in the wild-type suggests that the Schiff base forms a hydrogen bond, presumably with water402, in D212N(free) even upon neutralization of Asp212. The pair of bands at 2292 (−)/2265 (+) cm^{-1} disappeared in Figure 6b, suggesting the absence of the hydrogen-bonding alteration of Arg82. We infer that retinal photoisomerization does not cause structural change in Arg82 because of the weakened hydrogen-bonding network of the pentagonal cluster structure (Figure 1).

The spectral features in the 2300−2100 cm^{-1} region are hardly changed by halide binding (Figure 6c−e), showing a negative peak at 2212 cm^{-1} for D212N(Cl^-) and (Br^-), and at 2214 cm^{-1} for D212N(I^-). These peaks are likely to originate from the N−D stretch of the Schiff base, and little halide dependence clearly indicates that halide is not a hydrogen-bonding acceptor of the protonated Schiff base. The present observation for D212N is entirely different from that for D85S. In the latter case, the strongest negative peak appears at 2166 cm^{-1} for D85S(Cl^-), 2209 cm^{-1} for D85S(Br^-), and 2255 cm^{-1} for D85S(I^-), and such strong halide dependence shows a direct hydrogen bond of the Schiff base with halide (*27*). This present observation is consistent with the preceding analysis of the C=N stretch of the Schiff base (Figure 5).

In contrast to the Schiff base vibration, a prominent change in the spectral features was observed for the water bands at 2350−2300 cm^{-1}. While no water bands are observed for halide-free D212N (Figure 6b), halide binding to D212N induces the appearance of strongly hydrogen-bonded water molecules. In fact, water bands were observed at 2347 (−)/2312 (+) cm^{-1} for D212N(Cl^-) (Figure 6c) and D212N(Br^-) (Figure 6d). The frequencies were slightly downshifted for D212N(I^-) (Figure 6e). Identical frequencies for Cl^- and Br^- suggest that such a strongly hydrogen-bonded water molecule does not form a direct hydrogen bond with halide, while halide binding itself lowers the frequency of vibrations of the water molecule. It should be noted that, from the comprehensive studies of water vibrations of various rhodopsins, we found that strongly hydrogen-bonded water molecules are always present in the rhodopsins exhibiting proton-pumping activity (*28*). Therefore, we recently hypothesized that strongly hydrogen-bonded water molecule(s) is required for the proton-pumping function of rhodopsins. The present observation is also consistent with our hypothesis, because halide-free D212N (no proton pumping) has no such water, but halide-bound D212N (proton pump) does possess a strongly hydrogen-bonded water molecule.

Figure 7 compares O−D stretching vibrations of water molecules in the 2730−2380 cm^{-1} region, which correspond to moderately or weakly hydrogen-bonded water molecules. While strongly hydrogen-bonded water O−D stretches

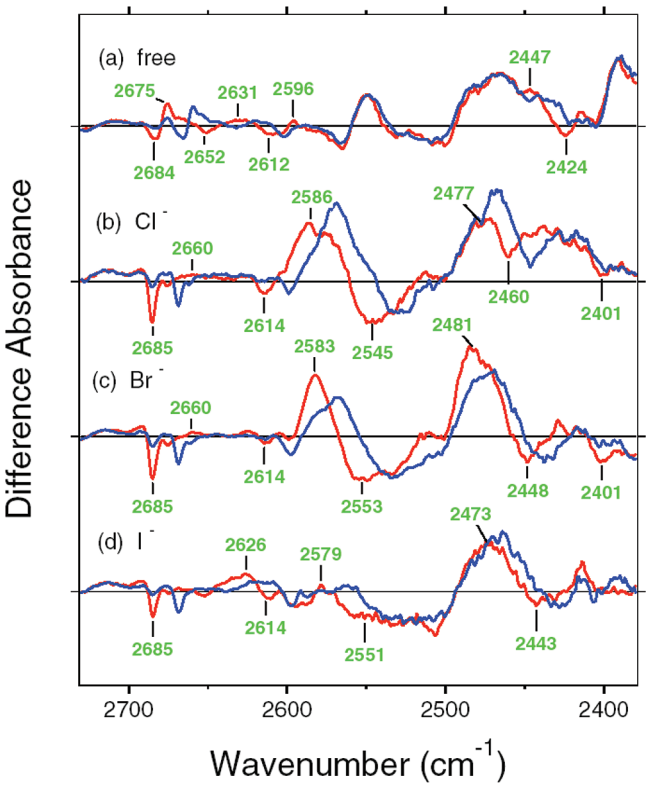

FIGURE 7: The K minus BR difference infrared spectra of halide-free (a), Cl^--bound (b), Br^--bound (c), and I^--bound (d) D212N in the 2730−2380 cm^{-1} region. The samples were hydrated with D_2O (red curves) or $D_2{}^{18}O$ (blue curves), and spectra were measured at 77 K. Green-labeled frequencies correspond to those identified as O−D stretching vibrations of water. One division of the *y*-axis corresponds to 0.0017 absorbance unit.

completely disappeared for halide-free D212N (Figure 6b), three negative (2684, 2652, and 2612 cm^{-1}) and three positive (2675, 2631, and 2596 cm^{-1}) bands were identified as the O−D stretches of water molecules at 2700−2600 cm^{-1} along with a pair of peaks at 2447 (+)/2424 (−) cm^{-1} (Figure 7a). Since the wild-type also possesses three negative (2684, 2652, and 2612 cm^{-1}) and three positive (2684, 2652, and 2612 cm^{-1}) bands in the same frequency region (*22*, *24*), we infer that the water-containing hydrogen-bonding network in the Schiff base region is also preserved in D212N-(free).

Figure 7 panels b−d show the spectra of halide-bound D212N, whose spectral features are similar for the three halides, but different from D212N(free) (Figure 7a). We identified the water bands at 2685 (−), 2660 (+), 2614 (−), 2586 (+), 2545 (−), 2477 (+), 2460 (−), and 2401 (−) cm^{-1} for D212N(Cl^-) (Figure 7b). Among the 5 negative bands, the bands at 2685 and 2614 cm^{-1} were completely halide independent, while the frequencies of the bands at 2545 and 2460 cm^{-1} were altered by 10 and 20 cm^{-1}, respectively, in a halide dependent manner. The band at 2401 cm^{-1} (Figure 7b) was also observed for D212N(Br^-) (Figure 7c), but its position is not clear for D212N(I^-) because of the noisy spectra (Figure 7d). We thus observed six negative bands of water for D212N(Cl^-) and D212N(Br^-), which is also the case for the wild-type (*24*). On the basis of comprehensive mutation study, we concluded that six water O−D stretches of the wild-type originate from three water molecules (water 401, 402, and 406) involved in the pentagonal cluster (Figure

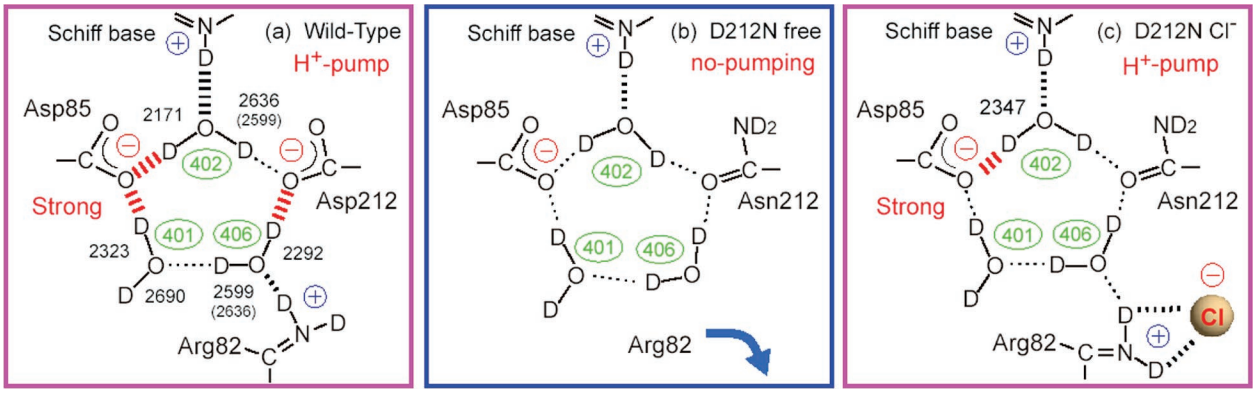

FIGURE 8: Schematic drawing of the structure of the deuterated Schiff base region in the wild-type (a), halide-free D212N (b), and Cl^--bound D212N (c). There are no strongly hydrogen-bonded water molecules in the halide-free D212N (b), whereas the strongly hydrogen-bonded water is present in the wild-type (a) and Cl^--bound D212N (c) that possess proton-pumping activity.

1) (*24*). Because of the similar FTIR spectra of the halide-bound D212N and weak halide dependence (Figure 4b), it is likely that halide-bound D212N has three water molecules in the Schiff base region similar to the wild-type, though hydrogen-bonding strengths of water are weaker than in the wild-type.

DISCUSSION

In this paper, we studied halide-bound D212N mutant of BR in detail. Light-induced pH changes in a suspension of proteoliposomes containing D212N at pH 5 clearly showed that chloride binding restores its proton-pumping activity. Spectral blue-shift by halide binding to D212N indicates that halide affects the counterion of the protonated Schiff base, but the halide dependence on the λ_{max} was much smaller for D212N (difference by 2.7 nm) than that for D85T (11 nm) (*43*). This fact suggests that the halide-binding site is distant from the chromophore in D212N. In the case of bromide-bound D85S mutant, X-ray crystallographic structure shows that Br^- is in direct hydrogen-bonding distance from the Schiff base (*44*), which is consistent with our FTIR investigation (*27*). Although there are no X-ray structures available for the D212N mutants, the present FTIR study provided useful structural information.

The K minus BR difference FTIR spectra of D212N at 77 K exhibit negligible halide dependence for vibrational bands of retinal and protein. Almost complete absence of halide dependence of the Schiff base vibrations strongly suggests that halide is not a direct hydrogen-bonding acceptor of the Schiff base, unlike in the case of D85S. On the other hand, halide-dependent bands were observed for the C=N stretch of Arg82 and some O−D water stretches, suggesting that these groups contribute to the halide-binding pocket. A strongly hydrogen-bonded water molecule is observed for the halide-bound D212N, but not for halide-free D212N, which is consistent with our hypothesis that such a water molecule is a prerequisite for proton-pumping activity of rhodopsins (*28*). On the basis of the present results, we try to construct the structural models of the Schiff base region of D212N in the absence and presence of halide, explaining why only the latter possesses proton-pumping activity (Figure 8).

The Schiff Base Structure of Halide-Free D212N. The N−D stretch of the Schiff base of D212N(free) at 2204 cm^{-1} is similar in frequency to that of the wild-type (Figure 6). Therefore, the Schiff base forms a hydrogen bond even upon neutralization of Asp212. The hydrogen-bonding acceptor is most likely to be water. In Figure 8, we propose that such a bridge water (similar to water402) is preserved in D212N-(free). X-ray crystallography of D85S(free) reported that the hydrogen-bonding acceptor of the Schiff base is a water molecule as well (*52*, *53*). In spite of the presence of the bridged water402, we did not experimentally observe hydrogen-bonding alteration of a strongly hydrogen-bonded water (<2400 cm^{-1}) (Figure 6b). One possibility is that there is no frequency change for the strongly hydrogen-bonded water, even though it is present in the active site. However, it is quite unlikely, because the Schiff base moves upon the retinal photoisomerization. Therefore, the O−D stretches of water402 in D212N(free) (Figure 8b) are presumably at >2400 cm^{-1}. It should be noted that the X-ray crystallographic structure of *Anabaena* sensory rhodopsin (ASR) showed the presence of such a bridged water between the Schiff base and Asp75 (*54*), but the O−D stretching frequencies are located at >2500 cm^{-1} (*33*). This was explained in terms of less preferable orientation for the hydrogen bond.

We observed four O−D stretching vibrations of water for D212N(free), indicating that at least two water molecules change their hydrogen bonds (Figures 6 and 7). According to our structural model (Figure 8b), three water molecules in the pentagonal cluster are preserved, but the hydrogen-bonding network is considerably weakened. A key reason is the neutralization of the negative charge at the position 212. In addition, the position of Arg82 must be important. Asp212 and Arg82 contribute to the quadrupole in the Schiff base region of the wild-type, where water406 is the bridged water between them (Figure 8a). The O−D stretch at 2292 cm^{-1} comes from a water molecule under strong hydrogen-bonding conditions (*22*, *24*). Lack of a negative charge at position 212 may move Arg82 toward the extracellular side. In fact, the pair of peaks assigned to Arg82 at 2292 (−)/2265 (+) cm^{-1} disappeared in Figure 6b, suggesting the absence of hydrogen-bonding alteration of Arg82. Retinal photoisomerization does not cause structural change in Arg82 in D212N(free), presumably because of (i) a weakened hydrogen-bonding network of the pentagonal cluster structure, and (ii) movement of Arg82 out of the Schiff base region (Figure 8b). X-ray crystallography of D85S(free) observed that the neutralization of Asp85 caused movement of Arg82 toward the extracellular side (*52*, *53*).

The Schiff Base Structure of Halide-Bound D212N. Halide binding restores the proton-pumping function for D212N, in contrast to the case of D85T or D85S. Halide binds in the direct hydrogen-bonding acceptor position in D85S, so that the light-induced protein structural changes drive the motion of halide (*44*). On the other hand, halide does not bind in the direct hydrogen-bonding acceptor position in D212N. Rather, halide binds near Arg82 in the Schiff base region (Figure 8c). In other words, halide binding causes the movement of Arg82 back into the Schiff base region. In fact, we observed halide-dependent vibrations at 1680−1660 cm^{-1} (Figure 5a), which can be most likely interpreted as C═N stretch of Arg82 (*48*−*50*). However, it appears that the C═O stretch of Asn212 is halide independent (Figure 5), suggesting that halide does not bind to Asn212.

We observed six O−D stretching vibrations of water for D212N(Cl^-) and D212N(Br^-), similar to the wild-type, indicating that three water molecules are involved in hydrogen-bonding alteration (Figures 6 and 7). Therefore, three water molecules probably constitute a pentagonal cluster structure in the halide-bound D212N (Figure 8c), like in the wild-type (Figure 8a). An important observation was the appearance of a strongly hydrogen-bonded water molecule for the halide-bound D212N, where the O−D stretch is located at 2347 cm^{-1} for D212N(Cl^-) and D212N(Br^-), and at 2338 cm^{-1} for D212N(I^-) (Figure 6). Identical frequencies of this band for Cl^- and Br^- suggest that this water molecule does not form a direct hydrogen bond with halide. In our model (Figure 8c), we propose that halide binding near Arg82 reconstitutes a pentagonal cluster structure, in which water402 forms a strong hydrogen bond with Asp85 in the wild-type-like fashion. The stretching frequency for this water (2347 cm^{-1}) is much higher than in the wild-type (2171 cm^{-1}), but it is sufficient to restore the proton pumping. The present model emphasizes the importance of (i) electrostatic interactions in the Schiff base region, particularly a quadrupolar structure, and (ii) a water-containing hydrogen-bonding network. Regarding the former, the importance of charge balance should be particularly noted, because the R82Q/D212N mutant pumps protons (*55*), and possesses strongly hydrogen-bonded water molecules (*24*). The charge balance must be important for the rearrangement of water molecules to form the strong hydrogen bond in the Schiff base region. Such rearrangement of hydrogen-bonding network presumably leads to the halide-dependent λ_{max} (difference of 2.7 nm; Figure 3), where the dipole between halide and Arg82 directly influences the chromophore, or the interaction between the chromophore and Asp85 is altered in a halide-dependent manner.

Role of Water Molecules in the Schiff Base Region for the Proton-Pumping Function. Figure 8 shows similar arrangements of structural components of the Schiff base region, but only the wild-type (Figure 8a) and halide-bound D212N (Figure 8c) pump protons. D212N(free) does not pump protons even in the presence of the proton donor (the Schiff base), acceptor (Asp85), and an intervening water molecule (water402) (Figure 8b). Why does not D212N(free) pump protons? Stretching frequencies of water molecules may give us a hint. The lowest frequency of water O−D stretch was observed at 2424 cm^{-1} for D212N(free), which we assumed to be the O−D stretch of water402 interacting with Asp85. Although the frequency difference between the absence (2424 cm^{-1}) and the presence (2347 cm^{-1}) of halide is only about 80 cm^{-1}, it may be essential.

We previously reported that, among various BR mutants, only D85N, D85S, and D212N lack strongly hydrogen-bonded water molecules (O−D stretch at $<$2400 cm^{-1}) and proton-pumping activity (*23*, *24*, *27*). Therefore, we proposed a hypothesis that the presence of a strong hydrogen bond of water is a prerequisite for proton pumping in rhodopsins (*28*). We have extensively tested this hypothesis for various rhodopsins by measuring O−D stretches of water. We found a perfect correlation between the presence of strongly hydrogen-bonded water molecule(s) and proton-pumping activity. For example, strongly hydrogen-bonded water molecules are observed for *pharaonis* phoborhodopsin (*29*), proteorhodopsin (*35*), *Leptosphaeria* rhodopsin (*37*), and azide-bound halorhodopsin (*32*), which all pump protons. Strongly hydrogen-bonded water molecules were not observed for *salinarum* halorhodopsin (*30*), *pharaonis* halorhodopsin (*30*, *31*), *Anabaena* sensory rhodopsin (*33*), *Neurospora* rhodopsin (*36*), and bovine rhodopsin (*56*), which have no proton-pumping acitivity. Cl^- pumping D85S has no strongly hydrogen-bonded water molecules as well (*27*). Thus, hydrogen-bonding strength of water molecules seems to be very important for the proton-pumping function. It should be noted that photon energy is stored first in its isomerized form. In addition to the distorted chromophore, the importance of a hydrogen-bonding network has to be emphasized for light-energy storage. Since only about 10% of light energy is spent on the electrochemical potential of transporting a proton (*57*), a small energy difference in hydrogen-bonding stabilization may be crucial for the pumping function.

Our hypothesis and its successful application to various rhodopsins have provided a concept for the new roles of internal water molecules. One of the important roles of internal water molecules is to occupy the empty space inside protein that may be energetically unfavorable. Internal water molecules may assist the transport of ions inside protein by raising dielectric constant (*8*). In addition, we showed the possibility that the hydrogen bond of water carries energy for the proton-pumping function, which can be monitored by FTIR spectroscopy.

REFERENCES

1. Haupts, U., Tittor, J., and Oesterhelt, D. (1999) Closing in on bacteriorhodopsin: Progress in understanding the molecules, *Annu. Rev. Biophys. Biomol. Struct. 28*, 367−399.
2. Lanyi, J. K. (2004) Bacteriorhodopsin, *Annu. Rev. Physiol. 66*, 665−688.
3. Mathies, R. A., Lin, S. W., Ames, J. B., and Pollard, W. T. (1991) From femtoseconds to biology: Mechanism of bacteriorhodopsin's light-driven proton pump, *Annu. Rev. Biophys. Biophys. Chem. 20*, 491−518.
4. Lanyi, J. K., and Váró, G. (1995) The photocycles of bacteriorhodopsin, *Isr. J. Chem. 35*, 365−385.
5. Siebert, F. (1990) Resonance Raman and infrared difference spectroscopy of retinal proteins, *Methods Enzymol. 189*, 123−136.
6. Krebs, M. P., and Khorana, H. G. (1993) Mechanism of light-dependent proton translocation by bacteriorhodopsin, *J. Bacteriol. 175*, 1555−1560.
7. Mogi, T., Stern, L. J., Marti, T., Chao, B. H., and Khorana, H. G. (1988) Aspartic acid substitutions affect proton translocation by bacteriorhodopsin, *Proc. Natl. Acad. Sci. U.S.A. 85*, 4148−4152.
8. Kandori, H. (2000) Role of internal water molecules in bacteriorhodopsin, *Biochim. Biophys. Acta 1460*, 177−191.

9. Luecke, H., Schobert, B., Richter, H.-T., Cartailler, J. P., and Lanyi, J. K. (1999) Structure of bacteriorhodopsin at 1.55 Å resolution, *J. Mol. Biol. 291*, 899−911.
10. Braiman, M. S., Mogi, T., Marti, T., Stern, L. J., Khorana, H. G., and Rothschild, K. J. (1988) Vibrational spectroscopy of bacteriorhodopsin mutant: Light-driven proton transport involves protonation changes of aspartic acid residues 85, 96, and 212, *Biochemistry 27*, 8516−8520.
11. Sasaki, J., Brown, L. S., Chon, Y.-S., Kandori, H., Maeda, A., Needleman, R., and Lanyi, J. K. (1995) Conversion of bacteriorhodopsin into a chloride ion pump, *Science 269*, 73−75.
12. Brown, L. S., Needleman, R., and Lanyi, J. K. (1996) Interaction of proton and chloride transfer pathways in recombinant bacteriorhodopsin with chloride transport activity: Implications for the chloride translocation mechanism, *Biochemistry 35*, 16048−16054.
13. Chon, Y.-S., Sasaki, J., Kandori, H., Brown, L. S., Lanyi, J. K., Needleman, R., and Maeda, A. (1996) Hydration of the counterion of the Schiff base in the chloride-transporting mutant of bacteriorhodopsin: FTIR and FT-Raman studies of the effects of anion binding when asp85 is replaced with a neutral residue, *Biochemistry 35*, 14244−14250.
14. Needleman, R., Chang, M., Ni, B., Váró, G., Fornés, J., White, S. H., and Lanyi, J. K. (1991) Properties of Asp^{212} → Asn bacteriorhodopsin suggest that Asp^{212} and Asp^{85} both participate in a counterion and proton acceptor complex near the Schiff base, *J. Biol. Chem. 266*, 11478−11484.
15. Moltke, S., Krebs, M. P., Mollaaghababa, R., Khorana, H. G., and Heyn, M. P. (1995) Intramolecular charge transfer in the bacteriorhodopsin mutants Asp85→Asn and Asp212→Asn: Effects of pH and anions, *Biophys. J. 69*, 2074−2083.
16. Kandori, H., Kinoshita, N., Shichida, Y., and Maeda, A. (1998) Protein structural changes in bacteriorhodopsin upon photoisomerization as revealed by polarized FTIR spectroscopy, *J. Phys. Chem. B 102*, 7899−7905.
17. Kandori, H., Belenky, M., and Herzfeld, J. (2002) Vibrational frequency and dipolar orientation of the protonated Schiff base in bacteriorhodopsin before and after photoisomerization, *Biochemistry 41*, 6026−6031.
18. Kandori, H., Kinoshita, N., Yamazaki, Y., Maeda, A., Shichida, Y., Needleman, R., Lanyi, J. K., Bizounok, M., Herzfeld, J., Raap, J., and Lugtenburg, J. (1999) Structural change of threonine 89 upon photoisomerization in bacteriorhodopsin as revealed by polarized FTIR spectroscopy, *Biochemistry 38*, 9676−9683.
19. Kandori, H., Kinoshita, N., Yamazaki, Y., Maeda, A., Shichida, Y., Needleman, R., Lanyi, J. K., Bizounok, M., Herzfeld, J., Raap, J., and Lugtenburg, J. (2000) Local and distant protein structural changes on photoisomerization of the retinal in bacteriorhodopsin, *Proc. Natl. Acad. Sci. U.S.A. 97*, 4643−4648.
20. Kandori, H., Yamazaki, Y., Shichida, Y., Raap, J., Lugtenburg, J., Belenky, M., and Herzfeld, J. (2001) Tight Asp-85-Thr-89 association during the pump switch of bacteriorhodopsin, *Proc. Natl. Acad. Sci. U.S.A. 98*, 1571−1576.
21. Tanimoto, T., Shibata, M., Belenky, M., Herzfeld, J., and Kandori, H. (2004) Altered hydrogen bonding of Arg82 during the proton pump cycle of bacteriorhodopsin: A low-temperature polarized FTIR spectroscopic study, *Biochemistry 43*, 9439−9447.
22. Kandori, H., and Shichida, Y. (2000) Direct observation of the bridged water stretching vibrations inside a protein, *J. Am. Chem. Soc. 122*, 11745−11746.
23. Shibata, M., Tanimoto, T., and Kandori, H. (2003) Water molecules in the Schiff base region of bacteriorhodopsin, *J. Am. Chem. Soc. 125*, 13312−13313.
24. Shibata, M., and Kandori, H. (2005) FTIR studies of internal water molecules in the Schiff base region of bacteriorhodopsin, *Biochemistry 44*, 7406−7413.
25. Mizuide, N., Shibata, M., Friedman, N., Sheves, M., Belenky, M., Herzfeld, J., and Kandori, H. (2006) Structural changes in bacteriorhodopsin following retinal photoisomerization from the 13-cis form, *Biochemistry 45*, 10674−10681.
26. Tanimoto, T., Furutani, Y., and Kandori, H. (2003) Structural changes of water in the Schiff base region of bacteriorhodopsin: Proposal of a hydration switch model, *Biochemistry 42*, 2300−2306.
27. Shibata, M., Ihara, K., and Kandori, H. (2006) Hydrogen-bonding interaction of the protonated Schiff base with halides in a chloride-pumping bacteriorhodopsin mutant, *Biochemistry 45*, 10633−10640.
28. Furutani, Y., Shibata, M., and Kandori, H. (2005) Strongly hydrogen-bonded water molecules in the Schiff base region of rhodopsins, *Photochem. Photobiol. Sci. 4*, 661−666.
29. Kandori, H., Furutani, Y., Shimono, K., Shichida, Y., and Kamo, N. (2001) Internal water molecules of *pharaonis* phoborhodopsin studied by low-temperature infrared spectroscopy, *Biochemistry 40*, 15693−15698.
30. Shibata, M., Muneda, N., Ihara, K., Sasaki, T., Demura, M., and Kandori, H. (2004) Internal water molecules of light-driven chloride pump proteins, *Chem. Phys. Lett. 392*, 330−333.
31. Shibata, M., Muneda, M., Sasaki, T., Shimono, K., Kamo, N., Demura, M., and Kandori, H. (2005) Hydrogen-bonding alterations of the protonated Schiff base and water molecule in the chloride pump of *Natronobacterium pharaonis*, *Biochemistry 44*, 12279−12286.
32. Muneda, N., Shibata, M., Demura, M., and Kandori, H. (2006) Internal water molecules of the proton-pumping halorhodopsin in the presence of azide, *J. Am. Chem. Soc. 128*, 6294−6295.
33. Furutani, Y., Kawanabe, A., Jung, K.-H., and Kandori, H. (2005) FTIR spectroscopy of the all-trans form of *Anabaena* sensory rhodopsin at 77 K: Hydrogen bond of a water between the Schiff base and Asp75, *Biochemistry 44*, 12287−12296.
34. Kawanabe, A., Furutani, Y., Jung, K.-H., and Kandori, H. (2006) FTIR study of the photoisomerization processes in the 13-cis and all-trans forms of *Anabaena* sensory rhodopsin at 77 K, *Biochemistry 45*, 4362−4370.
35. Furutani, Y., Ikeda, D., Shibata, M., and Kandori, H. (2006) Strongly hydrogen-bonded water molecules is observed only in the alkaline form of proteorhodopsin, *Chem. Phys. 324*, 705−708.
36. Furutani, Y., Bezerra, A. G., Jr., Waschuk, S., Sumii, M., Brown, L. S., and Kandori, H. (2004) FTIR spectroscopy of the K photointermediate of *Neurospora* rhodopsin: Structural changes of the retinal, protein, and water molecules after photoisomerization, *Biochemistry 43*, 9636−9646.
37. Sumii, M., Furutani, Y., Waschuk, S. A., Brown, L. S., and Kandori, H. (2005) Strongly hydrogen-bonded water molecule present near the retinal chromophore of *Leptosphaeria* rhodopsin, bacteriorhodopsin-like proton pump from a eukaryote, *Biochemistry 44*, 15159−15166.
38. Peck, R. F., DasSarma, S., and Krebs, M. P. (2000) Homologous gene knockout in the archaeon *Halobacterium salinarum* with ura3 as a counterselectable marker, *Mol. Microbiol. 35*, 667−676.
39. Cline, S. W., and Doolittle, W. F. (1987) Efficient transfection of the archaebacterium *Halobacterium halobium*, *J. Bacteriol. 169*, 1341−1344.
40. Oesterhelt, D., and Stoeckenius, W. (1973) Isolation of the cell membrane of *Halobacterium halobium* and its fractionation into red and purple membrane, *Methods Enzymol. 31*, 667−678.
41. Racker, E., and Stoeckenius, W. (1974) Reconstitution of purple membrane vesicles catalyzing light-driven proton uptake and adenosine triphosphate formation, *J. Biol. Chem. 249*, 662−663.
42. Schobert, B., and Lanyi, J. K. (1982) Halorhodopsin is a light-driven chloride pump, *J. Biol. Chem. 257*, 10306−10313.
43. Tittor, J., Haupts, U., Haupts, C., Oesterhelt, D., Becker, A., and Bamberg, E. (1997) Chloride and proton transport in bacteriorhodopsin mutant D85T: Different modes of ion translocation in a retinal protein, *J. Mol. Biol. 271*, 405−416.
44. Facciotti, M. T., Cheung, V. S., Nguyen, D., Rouhani, S., and Glaeser, R. M. (2003) Crystal structure of the bromide-bound D85S mutant of bacteriorhodopsin: Principles of ion pumping, *Biophys. J. 85*, 451−458.
45. Marti, T., Rösselet, S. J., Otto, H., Heyn, M. P., and Khorana, H. G. (1991) The retinylidene Schiff base counterion in bacteriorhodopsin, *J. Biol. Chem. 266*, 18674−18683.
46. Krebs, M. P., Mollaaghababa, R., and Khorana, H. G. (1993) Gene replacement in *Halobacterium halobium* and expression of bacteriorhodopsin mutants, *Proc. Natl. Acad. Sci. U.S.A. 90*, 1987−1993.
47. Smith, S. O., Lugtenburg, J., and Mathies, R. A. (1985) Determination of retinal chromophore structure in bacteriorhodopsin with resonance raman spectroscopy, *J. Membr. Biol. 85*, 95−109.
48. Braiman, M. S., Briercheck, D. M., and Kriger, M. (1999) Modeling vibrational spectra of amino acid side chains in proteins: Effects of protonation state, counterion, and solvent on arginine C-N stretch frequencies, *J. Phys. Chem. B 103*, 4744−4750.
49. Xiao, Y., Hutson, M. S., Belenky, M., Herzfeld, J., and Braiman, M. S. (2004) Role of arginine-82 in fast proton release during

the bacteriorhodopsin photocycle: A time-resolved FT-IR study of purple membrane containing ^{15}N-labeled arginine, *Biochemistry 43*, 12809−12818.

50. Hutson, M. S., Alexiev, U., Shilov, S. V., Wise, K. J., and Braiman, M. S. (2000) Evidence for a perturbation of arginine-82 in the bacteriorhodopsin photocycle from time-resolved infrared spectra, *Biochemistry 39*, 13189−13200.
51. Yamazaki, Y., Tuzi, S., Saitô, H., Kandori, H., Needleman, R., Lanyi, J. K., and Maeda, A. (1996) Hydrogen bonds of water and C═O groups coordinate long-range structural changes in the L photointermediate of bacteriorhodopsin, *Biochemistry 35*, 4063−4068.
52. Rouhani, S., Cartailler, J.-P., Facciotti, M. T., Walian, P., Needleman, R., Lanyi, J. K., Glaeser, R. M., and Luecke, H. (2001) Crystal structure of the D85S mutant of bacteriorhodopsin: Model of an O-like photocycle intermediate, *J. Mol. Biol. 313*, 615−628.
53. Facciotti, M. T., Cheung, V. S., Lunde, C. S., Rouhani, S., Baliga, N. S., and Glaeser, R. M. (2004) Specificity of anion binding in the substrate pocket of bacteriorhodopsin, *Biochemistry 43*, 4934−4943.
54. Vogeley, L., Sineshchekov, O. A., Trivedi, V. D., Sasaki, J., Spudich, J. L., and Luecke, H. (2004) *Anabaena* sensory rhodopsin: a photochromic color sensor at 2.0 Å, *Science 306*, 1390−1393.
55. Brown, L. S., Váró, G., Hatanaka, M., Sasaki, J., Kandori, H., Maeda, A., Friedman, N., Sheves, M., Needleman, R., and Lanyi, J. K. (1995) The complex extracellular domain regulates the deprotonation and reprotonation of the retinal Schiff base during the bacteriorhodopsin photocycle, *Biochemistry 34*, 12903−12911.
56. Furutani, Y., Shichida, Y., and Kandori, H. (2003) Structural changes of water molecules during the photoactivation processes in bovine rhodopsin, *Biochemistry 42*, 9619−9625.
57. Birge, R. R. (1990) Nature of the primary photochemical events in rhodopsin and bacteriorhodopsin, *Biochim. Biophys. Acta 1016*, 293−327.

BI7004224